



## Variability of chlorophyll-*a* and diatoms in the frontal ecosystem of Indian Ocean sector of the Southern Ocean

Mishra RAJANI KANTA\*, Jena BABULA, Narayana Pillai ANILKUMAR,  
Naik RAVIDAS KRISHNA, Parli VENKATESWARAN BHASKAR  
and Soares MELENA A

National Centre for Antarctic and Ocean Research, Ministry of Earth Sciences (MoES),  
Vasco-da-Gama, Goa, India

\* corresponding author <rajanimishra@yahoo.com>

**Abstract:** Phytoplankton composition plays a major role in biogeochemical cycles of the ocean. The intensity of carbon fixation and export is strongly dependent on the phytoplankton community. Yet, the contribution of different types of phytoplankton to the total production on various communities is still poorly understood in the Indian Ocean sector of Southern Ocean (SO). Therefore the variability of chlorophyll-*a* (*Chl-a*) and diatoms in the frontal ecosystems of the Indian sector of SO have been investigated along with the sea surface temperature (SST), sea surface wind (SSW), photosynthetically active radiation (PAR), and nutrients datasets for the period of 1998–2012. Combined analysis of *in-situ*, model and satellite observations indicate that the variability of *Chl-a* and diatoms were primarily influenced by light and wind. The *Chl-a* was higher at the sub-Antarctic front (SAF) followed by the sub-tropical front (STF) and the polar front (PF). The diatom concentration was higher at the SAF followed by the PF and STF. Maximum concentration of *Chl-a* and diatoms commonly observed at the SAF region are probably due to the moderate PAR, SST and wind. Dominance of diatoms at the PF may be attributed to their adaptability for low light conditions. The results from this study in the frontal ecosystems would help to understand the biogeochemical cycle of the Indian sector of the SO.

Key words: Antarctic, Southern Ocean, chlorophyll-*a*, diatoms.

### Introduction

The Southern Ocean (SO) is an important component of the global carbon cycle with unique physical and chemical characteristics due to its connectivity to the entire World Ocean. The Polar Front (PF) is one of the major fronts

associated with the Antarctic Circumpolar Current (ACC). Other fronts within the ACC include the sub-Antarctic front (SAF) and the Sub-tropical front (STF) (Orsi *et al.* 1995). There is a strong gradient in sea surface temperature (SST) across the fronts especially at the PF region as it marks the transition between cold Antarctic surface water to the south and warmer sub-Antarctic surface waters to the north. Each SO front is an important boundary in terms of physical, chemical, and biological characteristics of the Ocean. The chlorophyll-*a* (*Chl-a*) concentrations in the SO are typically low despite the high concentrations of major nutrients in the surface waters and hence known as the High Nutrient Low Chlorophyll regions (HNLC) (Moore *et al.* 2002). Phytoplankton associated with the PF is typically dominated by diatoms species (Brown and Landry 2001; Salas *et al.* 2011). Unlike smaller phytoplankton, large diatoms are less susceptible to grazing by microzooplankton and typically have long reproductive times relative to the smaller celled species (Smetacek *et al.* 2004).

Among the various groups of phytoplankton the contribution of diatoms to the global primary production and planktonic food chain is very significant (Treguer *et al.* 1995). They dominate the phytoplankton throughout the Antarctic and Arctic Oceans and are responsible for the highest level of primary production under the nutrient replete conditions of the SO (Nelson *et al.* 1995). The thick accumulation of diatomaceous sediment on the SO sea floor shows their importance in the export of carbon to the deep ocean (Honjo *et al.* 2008). Diatoms utilize silicic acid to construct their cell walls and are partly controlled by its availability and distribution. The diatoms efficiency in the biological pump plays a crucial role in explaining paleoclimate and past oceanographic processes (Stoermer and Smol 1999). Studies of modern oceanic processes, ancient marine sediment cores and diatom ecology suggest that export and burial of diatoms has the potential to cause rapid changes in atmospheric CO<sub>2</sub> concentration. Diatoms are estimated to contribute up to 45% of global primary production (Mann 1999) making them a major player in global biogeochemical cycles. Several other characteristics about diatoms physiology give them an ecological advantage over other phytoplankton competitors in the polar oceans. In contrast to other phytoplankton species whose division cycles are strongly coupled with the diel light cycle, diatoms are capable of dividing their cells at any point during the day (Martin-Jezequel *et al.* 2000). These features of diatoms physiology observed *in-situ*, probably contribute to higher growth rates at high latitudes compared to other marine algae (Furnas 1991). The strong seasonal cycle, low solar radiation and strong mixed layer depths in the SO frontal regions contribute to the reduced chlorophyll concentrations and phytoplankton abundance over an annual cycle (Abbott *et al.* 2000). Phytoplankton blooms due to the sea ice melting in the SO are well known. Firstly sea ice melt releases fresh water that forms a buoyant surface layer, stratifying the water column, this inhibits vertical mixing and increases mean light level in a shallow surface mixed layer (Krikman and Bitz

2011). Secondly the melting ice provides a potentially considerable source of iron because of the winter accumulation of aeolian particles on the sea ice surface (Gao *et al.* 2003).

The SO is recognized as a sink and source for the atmospheric CO<sub>2</sub> over glacial-interglacial and seasonal climate cycles (Sigman and Boyle 2000), but there are uncertainties in the relative quantity and importance of different water masses in frontal regions to the physical, chemical and biological processes that drive CO<sub>2</sub> exchange (Sigman *et al.* 2010). To understand the distribution and ecology of diatoms in the surface sediments and how this is connected to the surface water, it is essential to establish reliable proxies of past sea surface conditions (Armand *et al.* 2005). Though the SO is an HNLC region, the *Chl-a* concentration and phytoplankton blooms have been observed in the vicinity of major SO fronts (Moore and Abbott 2002) and on meridional transects of the PF (Menglet *et al.* 2001). Within this context, little is known about the spatial frontal variability of both *Chl-a* concentration and abundance of diatom community over a long period in the Indian Ocean sector of SO. *In-situ* observations of *Chl-a* and diatoms are difficult to collect in the SO due to its remoteness and limited accessibility. Satellite remote sensing and long records of model-derived datasets are being used for assessing large-scale oceanic processes in the SO. The present study deals with the variability of chlorophyll-*a* (*Chl-a*) and diatoms in the frontal ecosystems of the Indian sector of SO, in response to the sea surface temperature (SST), sea surface wind (SSW), photosynthetically active radiation (PAR), and nutrients datasets using *in-situ* (2012) and model datasets (1998–2012).

## Methods

***In-situ* sampling.** — Extensive work has been carried out to identify the different frontal regions of the Southern Ocean (SO) using satellite and model analysed observations (Orsi *et al.* 1995; Holiday and Read 1998). While identifying the fronts, the discrepancy in the positions occurs because of diverse datasets and methodologies. Although the north-south movement of fronts are well known in the Southern Ocean, for the purpose of this study we have classified three frontal regions: the subtropical front (STF: 39°S–43°S), sub-Antarctic front (SAF: 45°S–48°S) and polar front (PF: 52°S–56°S) along the 53.5°E and 57.5°E meridian in the Indian Ocean sector of SO (Fig. 1).

A total of eight stations were sampled from the three frontal regions on board ORV *Sagar Nidhi* during the austral summer (Jan–Feb) of 2012 (Table 1). The water samples were collected using a rosette sampler from the surface water 1–5 m by the SBE CTD (SeaBird, USA) for the analysis of chlorophyll-*a*, diagnostic pigments and nutrients. The nutrients (nitrate, phosphate and silicate) were measured in an autoanalyzer, (Skalar Analytical San<sup>++</sup> 8505 interface V3.05,

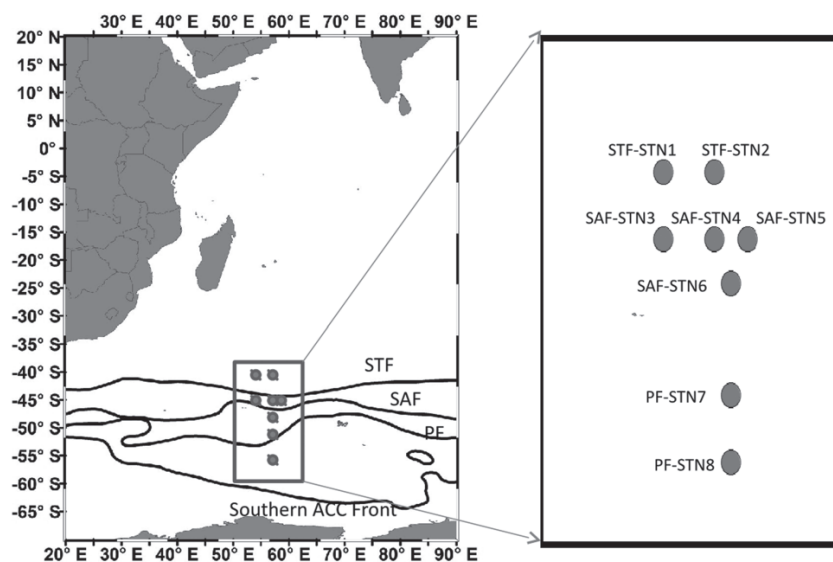


Fig. 1. In situ sampling locations from 2012. Stations 1 and 2 belong to the STF zone; stations 3–6 belongs to the SAF zone; stations 7, 8 belong to the PF zone.

Table 1

Detail of sampling dates and geographic location during the study period.

Station	Date	GMT Time	Latitude	Longitude	Variables measured
STN1	15/01/2012	18:20	40°S	56°30'	phytoplankton pigment (chlorophyll <i>a</i> ), diatoms pigment based, nutrients
STN2	16/01/2012	20:05	40°S	53°30'	phytoplankton pigment (chlorophyll <i>a</i> ), diatoms pigment based, nutrients
STN3	18/01/2012	00:00	43°S	53°30'	phytoplankton pigment (chlorophyll <i>a</i> )
STN4	18/01/2012	20:30	43°S	56°30'	phytoplankton pigment (chlorophyll <i>a</i> )
STN5	19/01/2012	10:15	43°S	58°30'	phytoplankton pigment (chlorophyll <i>a</i> )
STN6	20/01/2012	08:15	45°S	58°30'	phytoplankton pigment (chlorophyll <i>a</i> )
STN7	22/01/2012	05:32	50°S	57°30'	phytoplankton pigment (chlorophyll <i>a</i> ), diatoms pigment based, nutrients
STN8	23/01/2012	12:55	53°S	57°30'	phytoplankton pigment (chlorophyll <i>a</i> ), diatoms pigment based, nutrients

Netherlands), using standard protocols (Grasshoff *et al.* 1983). For the *Chl-a* and diagnostic pigment analysis, the samples were filtered through GF/F filters (nominal pore size 0.7  $\mu\text{m}$ ), extracted with 90% acetone overnight and analyzed against standard marker pigments by high performance liquid chromatography (HPLC) method (Van Heukelem and Thomas 2001). Abundance of diatoms was estimated based on the diagnostic pigments (DP) analysis as follows (Barlow *et al.* 2007)

$$\text{DP} = \text{PSC} + \text{Zea} + \text{Tchl-}b + \text{Allo} \quad (1)$$

where: *Zea* – Zeaxanthin, *Tchl-b* – Total chlorophyll *b* (sum of *chl-b* + *Dv chl-b*), *Allo* – Alloxanthin, and *PSC* is photosynthetic carotenoid pigments, which was further estimated as follows:

$$\text{PSC} = \text{But} + \text{Fuco} + \text{Hex} + \text{Peri} \quad (2)$$

*But* = 19' Butanoylx fucoxanthin, *Fuco* – Fucoxanthin, *Hex* – 19' Hexanoylo-fucoxanthin, *Peri* – peridinin.

The proportion of diatoms was estimated as:

$$\text{Diatom}_{\text{DP}} = \text{Fuco}/\text{DP} \quad (3)$$

**Satellite datasets and model analyses.** – Satellite datasets on monthly and annual average chlorophyll-*a* (*Chl-a*) concentrations, Sea Surface Temperature (SST), Sea Surface Wind (SSW), and Photosynthetic Available Radiation (PAR) were acquired from the National Aeronautics and Space Administration (NASA) data archive as specified details in Table 2. QuickSCAT wind vectors (25 km spatial resolution) and the Aqua-Moderate Resolution Imaging Spectro radiometer (MODIS) SST products were acquired from NASA Jet Propulsion Laboratory.

Table 2

Detail of satellite datasets used in the present study.

Parameters	Satellite sensor	Spatial resolution	Temporal resolution	Time span	Data source
Sea Surface Temperature	Aqua-MODIS	4 km	monthly	2000–present	JPL, NASA
Sea Surface Wind	QUIKSCAT	25 km	monthly	1999–2009	JPL, NASA
Chlorophyll- <i>a</i> and Photosynthetically Active Radiation	SeaWiFS and AquaMODIS	9 km and 4 km	monthly	1997–2010 and 2002–present	Ocean Colour NASA

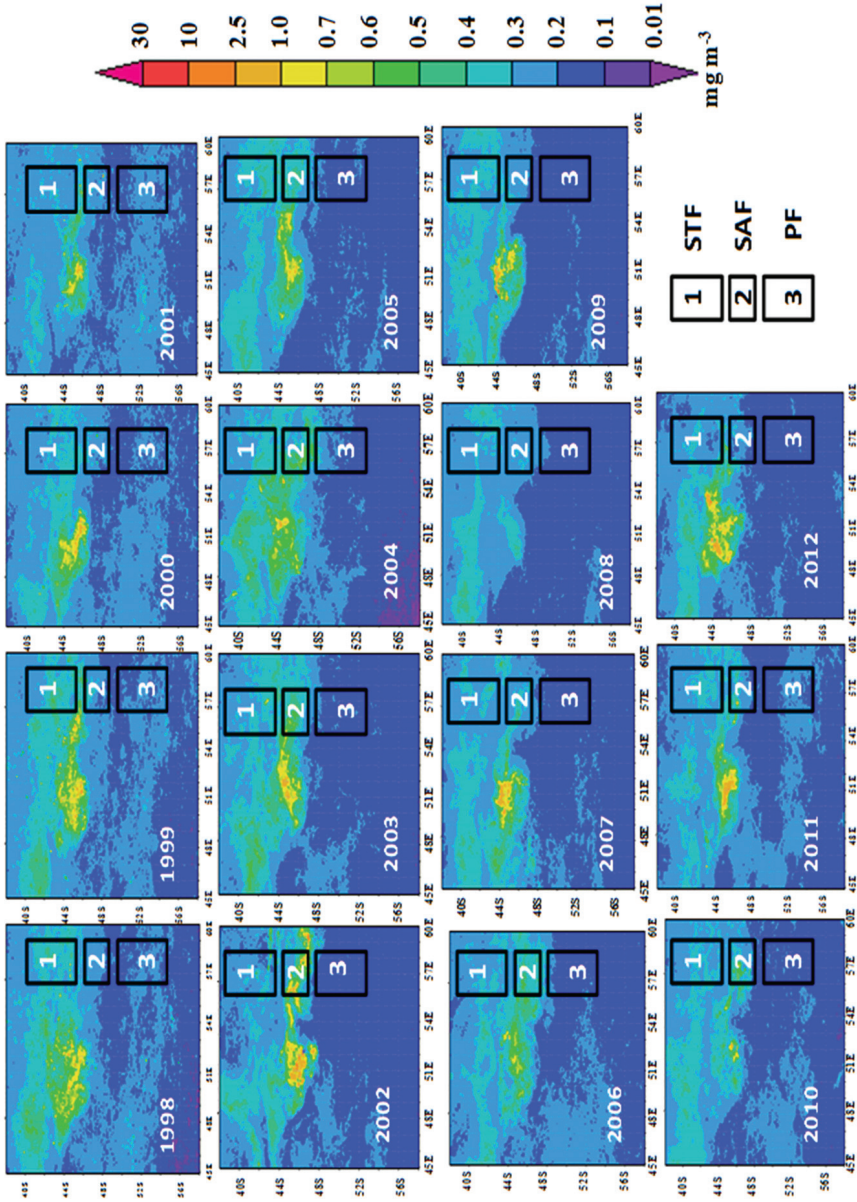


Fig. 2. Mean annual *Chl-a* concentration calculated from the combined SeaWiFS (1998–2002) and MODIS-Aqua (2003–2012) data sets. Insert boxes denote: 1: STF, 2: SAF, 3: PF. Figure produced using Giovanni, NASA-OBPG.

SeaWiFS (9 km spatial resolution) and MODIS (4 km spatial resolution) monthly products of *Chl-a* and PAR were acquired from the Ocean Biology Processing Group (OBPG), Goddard Space Flight Center. These products were used as input for running the NASA Ocean Biogeochemical Model (NOBM), along with *in situ* observations. Monthly and annual averages on *Chl-a*, diatom concentrations ( $0.667 \times 1.25^\circ$  spatial resolution) and nitrate products ( $0.5 \times 0.625^\circ$  spatial resolution) from the model analysed field (NOBM) were used in the present study during 1998–2012. This model is based on 14 vertical layers in quasi-isopycnal coordinates, driven by wind stress, SST, shortwave radiation and the ocean general circulation model (OGCM), and has been extensively validated with *in-situ* based nutrients and chlorophyll (Gregg *et al.* 2003). In this work we have performed comparative analysis of *in situ* observations, satellite datasets, and model output field as shown in Fig. 2.

## Results

**Variability of *Chl-a* and diatoms.** — The values of *Chl-a* and diatoms concentrations averaged annually and within the three frontal regions (as delimited in this study) for the period 1998–2012 were computed (Figs 2 and 3). There was a general decline in *Chl-a* concentration from the SAF ( $0.28 \pm 0.038 \text{ mg m}^{-3}$ ) to the STF ( $0.26 \pm 0.032 \text{ mg m}^{-3}$ ) and the PF ( $0.177 \pm 0.014 \text{ mg m}^{-3}$ ) as shown in Fig. 3. However, the diatoms abundance declined from the SAF ( $0.24 \pm 0.014 \text{ mg m}^{-3}$ ) to the PF ( $0.176 \pm 0.012 \text{ mg m}^{-3}$ ) and STF ( $0.11 \pm 0.033 \text{ mg m}^{-3}$ ). In the STF, the highest *Chl-a* of  $0.328 \text{ mg m}^{-3}$  was observed during 2004; while at the SAF the highest *Chl-a* of  $0.330 \text{ mg m}^{-3}$  was observed during 2010; and at the PF the highest *Chl-a* of  $0.208 \text{ mg m}^{-3}$  was observed during 2001. Coincidentally at the STF, the highest concentrations of diatoms ( $0.175 \text{ mg m}^{-3}$ ) were recorded during 2004, whilst the highest diatoms concentrations at the SAF ( $0.260 \text{ mg m}^{-3}$ ) and at the PF ( $0.204 \text{ mg m}^{-3}$ ) occurred during 2010 and 2001, respectively.

Analysis of *in situ* observations collected during February 2012 indicated that *Chl-a* was highest at the SAF ( $0.81 \text{ mg m}^{-3}$ ) followed by the PF ( $0.615 \text{ mg m}^{-3}$ ) and the STF ( $0.48 \text{ mg m}^{-3}$ ) as shown in Fig. 4. Similarly the diatoms dominance was greatest in the PF region with diagnostic pigment (DP) index of 0.59 compared to the STF region (0.06). Unfortunately there is no *in-situ* data on diatoms index' because of the lack of pigment samples for this location. Model results for *Chl-a* and diatom concentrations follow the same distributional pattern at the fronts as the *in-situ* data.

**Variability of nitrate.** — Modelled nitrate concentrations showed large variations between the fronts with highest concentrations at the PF ( $5.03 \pm 0.234 \text{ } \mu\text{M L}^{-1}$ ) followed by the SAF ( $3.42 \pm 0.145 \text{ } \mu\text{M L}^{-1}$ ) and STF

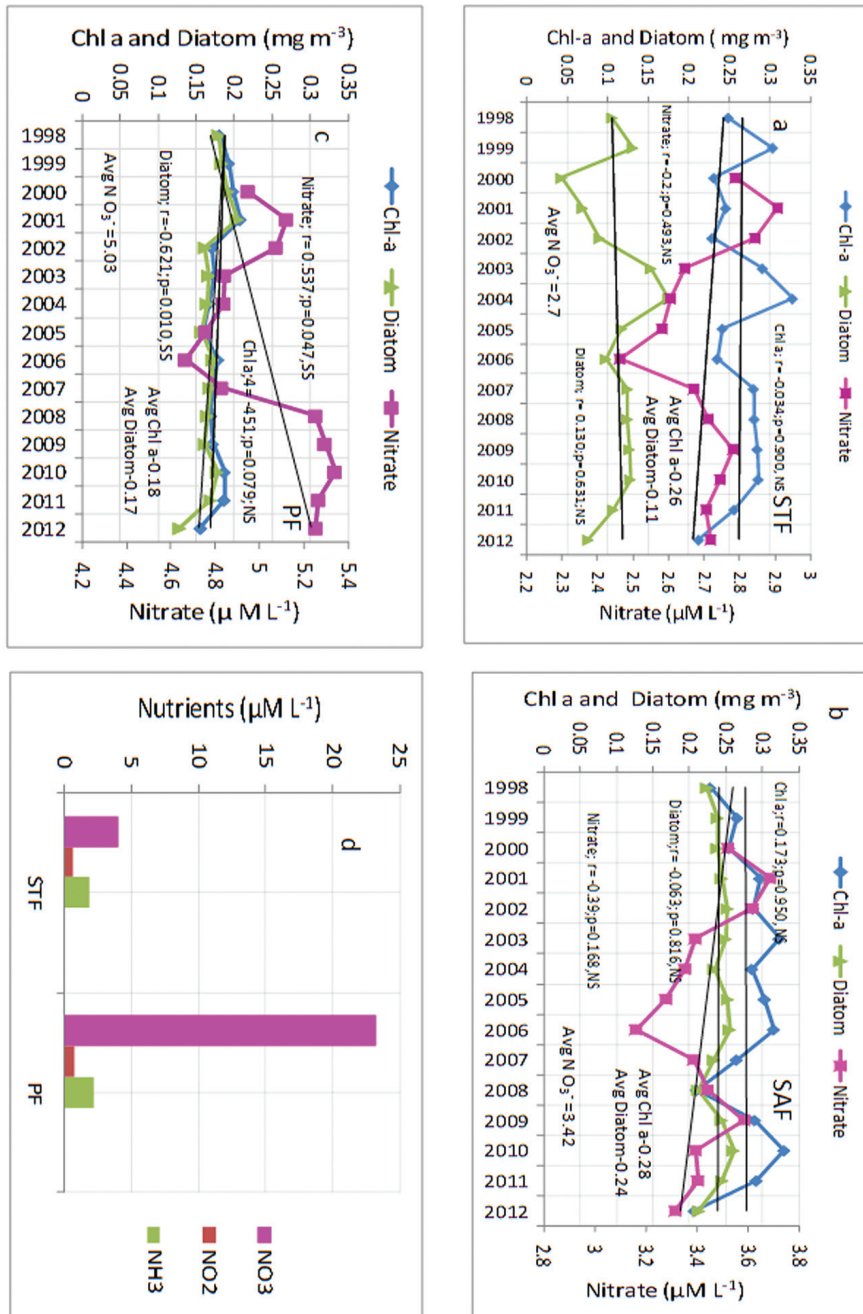


Fig. 3. a–c, Model retrievals of total *Chl-a*, diatoms and nitrate concentrations from 1998 to 2012; d, *in situ* nitrate concentrations at stations in the STF and PF zones during 2012.

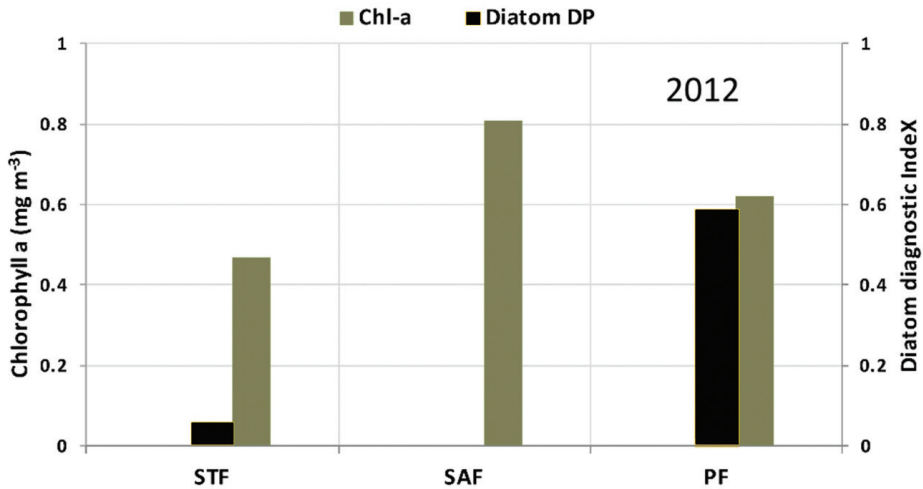


Fig. 4. The primary vertical axis shows *in situ* Chl-*a* concentrations and secondary vertical axis shows *in-situ* diatoms diagnostic Index at the STF, SAF and PF during 2012.

( $2.7 \pm 0.112 \mu\text{M L}^{-1}$ ) as shown in Fig. 3. At the STF and SAF, the peak of nitrate concentrations were recorded during 2001, while at the PF the peak concentration was observed during 2010. The nitrate level remained above  $2.4 \mu\text{M L}^{-1}$  in all frontal regions (Fig. 3a–c). The nitrate concentration shows the negative relationship with Chl-*a* and diatom at STF ( $r = -0.2$ ) and SAF ( $r = -0.063$ ) regions, whereas the positive relationship at PF ( $r = 0.537$ ), indicating no role/influence of nitrate in the low/high concentration of Chl-*a* and diatoms in the PF region. At the PF, the *in-situ* nitrate concentrations were 5 times higher than the model output (Fig. 3c,d). Similarly the *in-situ* values were 2 times higher than the model output at the STF region (Fig. 3a,d). The result suggests overall underestimation tendency of model output compared to *in-situ* observations. The observed discrepancy between model and *in situ* observations could be due to the difference in sampling time period. Model results are monthly average values; however *in-situ* observations are single measurement in a given time of the day.

**Variability of sea surface temperature (SST).** — Annual average of SST were highest at the STF ( $15.52 \pm 0.35^\circ\text{C}$ ) followed by the SAF ( $6.77 \pm 0.38^\circ\text{C}$ ) and PF ( $1.75 \pm 0.24^\circ\text{C}$ ) as shown in Fig. 5. At the STF the temperature was highest during 2001 ( $16.19^\circ\text{C}$ ) followed by 2007 ( $15.85^\circ\text{C}$ ) and lowest in 2009 ( $14.85^\circ\text{C}$ ). At the SAF the SST was highest in 2001 ( $7.21^\circ\text{C}$ ) followed by 2010 ( $6.9^\circ\text{C}$ ) and lowest in 2009 ( $5.81^\circ\text{C}$ ). At the PF, the SST was highest during 2001 ( $2.15^\circ\text{C}$ ) followed by 2002 ( $2.13^\circ\text{C}$ ) while the lowest was in 2006 ( $1.45^\circ\text{C}$ ). The greatest inter-annual SST variation at the STF was  $1.5^\circ\text{C}$  followed by SAF ( $1.4^\circ\text{C}$ ) and PF ( $0.9^\circ\text{C}$ ). SST strongly decreased from 2001 to 2006 and

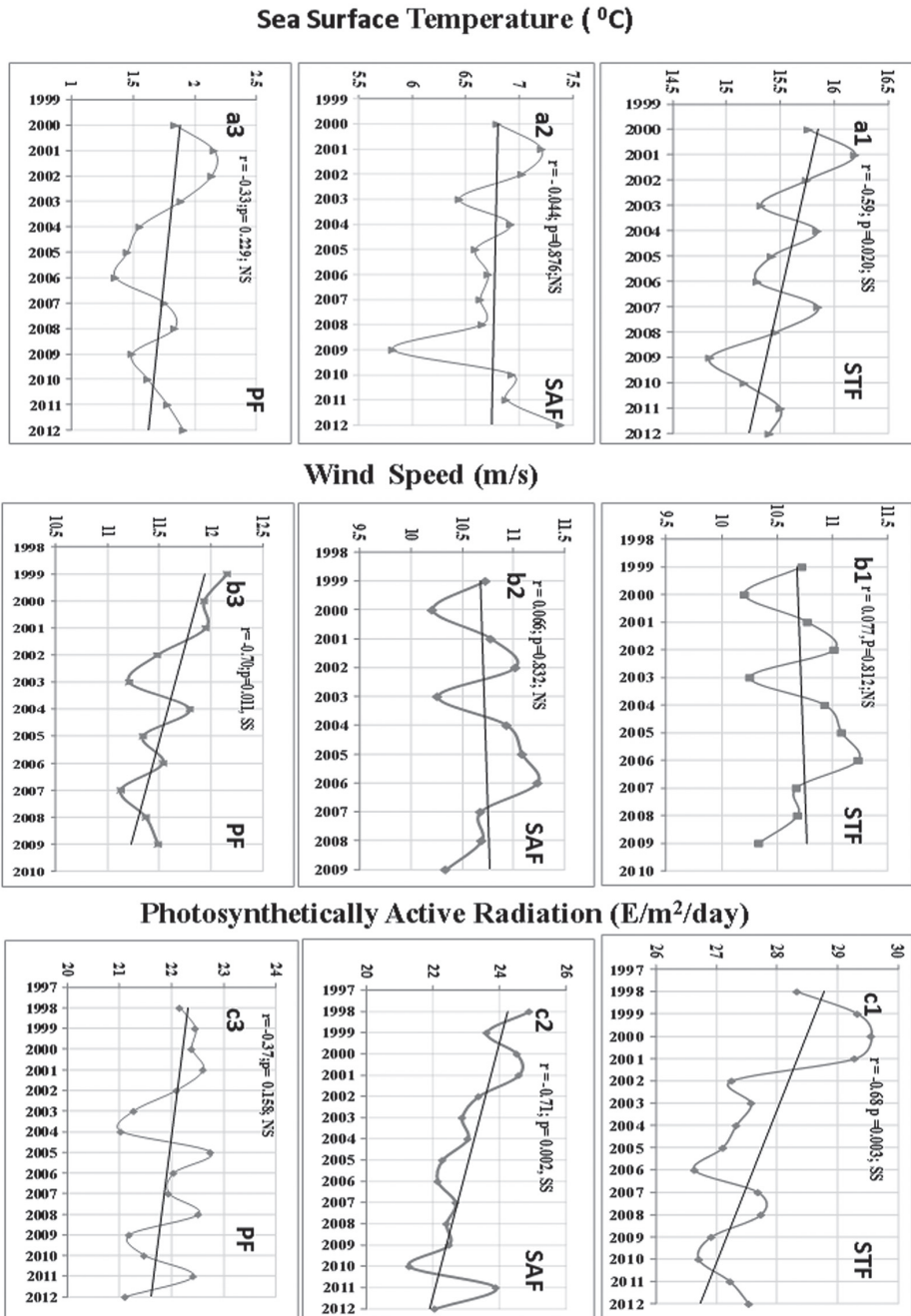


Fig. 5. Model retrievals of mean annual SST (a1–a3), SSW (b1–b3) and PAR (c1–c3) of different fronts of Indian sector of Southern Ocean.

increased from 2010 to 2012, however the entire trend was decreased at STF and PF (Fig. 5a1–a3). Whereas there was a single year (2009) notably cooler SST in the SAF and no obvious trend was found between 1998 and 2012.

**Variability of photosynthetic available radiation (PAR).** — The annual average of PAR decreased from the STF to the PF through the SAF, as expected due to the latitudinal change, as shown in Fig. 5. The inter-annual variation was highly significant during 1998–2012 in different frontal regions. The PAR was highest at STF ( $28 \pm 0.95 \text{ E m}^{-2}\text{day}^{-1}$ ) followed by SAF ( $23 \pm 1.04 \text{ E m}^{-2}\text{day}^{-1}$ ) and PF ( $21.75 \pm 0.98 \text{ E m}^{-2}\text{day}^{-1}$ ). At STF, the highest PAR was  $29.56 \text{ E m}^{-2}\text{day}^{-1}$  in 2000 and the lowest was  $27.53 \text{ E m}^{-2}\text{day}^{-1}$  in 2006. At SAF, the maximum PAR was  $24.89 \text{ E m}^{-2}\text{day}^{-1}$  in 1998 and the minimum was  $20.2 \text{ E m}^{-2}\text{day}^{-1}$  in 2010. At PF, the highest PAR was  $22.71 \text{ E m}^{-2}\text{day}^{-1}$  in 2005 and the lowest was in 2004 ( $21.03 \text{ E m}^{-2}\text{day}^{-1}$ ). The average PAR distribution was greatly followed by the distribution of *Chl-a* and diatoms across all the fronts with positive correlations. The PAR had significant correlations (Fig. 6) with *Chl-a* ( $r = 0.82$ ;  $p = 0.0001$ ) at PF followed by SAF ( $r = 0.67$ ;  $p = 0.0001$ ) and STF ( $r = 0.50$ ;  $p = 0.0001$ ). Similarly the PAR had a significant correlations with diatoms ( $r = 0.82$ ;  $p = 0.0001$ ) at PF followed by SAF ( $r = 0.50$ ;  $p = 0.0001$ ) and STF ( $r = 0.16$ ;  $p = 0.0491$ ). The correlation between PAR and SST at STF was 0.82, at PF was 0.93 and at SAF was 0.68, respectively.

**Variability of wind speed.** — The annual average of SSW declined northwards across the fronts with highest recorded at the PF and lowest wind speeds at the STF. Between 1998 and 2009 the SSW speeds decreased in the PF region, whereas it increased in the SAF and STF over the same period. The amplitude of change was also the highest at PF. At the STF region the greatest average wind speeds were observed during 2007 ( $10.43 \pm 1.22 \text{ m/s}$ ) followed by 2005 ( $10.35 \pm 1.17 \text{ m/s}$ ) and the lowest during 2000 ( $9.31 \pm 1.05 \text{ m/s}$ ) as shown in Fig. 5. At the SAF, the highest average wind speeds occurred during 2006 ( $11.23 \pm 0.15 \text{ m/s}$ ) and lowest during 2000 ( $10.42 \pm 0.35$ ) as shown in Fig. 5. At the PF, highest average wind speeds were recorded during 1999 ( $12.15 \pm 0.23 \text{ m/s}$ ) and lowest average during 2007 ( $11.21 \pm 0.35 \text{ m/s}$ ) as shown in Fig. 5.

The monthly statistical relationship between the biological parameters (*Chl-a* and diatoms) and PAR, wind, SST and nitrate are shown in Figs 6 and 7. The result reveals that *Chl-a* and diatoms variability is dominantly influenced by PAR at the PF ( $r = 0.82$ ;  $p = 0.0001$ ) followed by SAF and STF (Figs 6 and 7). In general, significant negative relationship was observed between wind and these biological parameters (*Chl-a* and diatoms). SST showed significant relationship with *Chl-a* and diatoms at PF and at STF, but not at SAF. Nitrate showed significant relationship with *Chl-a* and diatoms, only at the STF and SAF.

## Discussion

The highest average *Chl-a* concentration and diatom abundance were observed at the SAF showing several peaks between 1998 and 2012. A most plausible explanation would be that the moderate wind speed (annual average calculated from weak and strong wind speed of individual months of a particular year) at the SAF facilitate a thorough mixing at the surface of the ocean, which results in the accumulation/growth of phytoplankton biomass (*Chl-a*) and particularly diatom abundance in this frontal region as compared to the STF and the PF. As the wind speed increases the mixed layer deepens, stratification decreases and the mean light level available to phytoplankton decreases. In contrast, weaker winds result in an increase in stratification, and a well illuminated shallower mixed layer. On the other hand, weaker winds may limit the input of iron. Although the PF experiences higher average winds speeds (and therefore greater mixed layer depth and reduced light availability), the influence of sea ice melt to support surface stratification and increase iron availability may offset the wind effect compared to the SAF (Fitch and Moore 2007).

*Chl-a* concentration and diatom abundance showed large scale variations at the different frontal regions due to changes in the environmental conditions (Mishra *et al.*, 2015, 2017). PAR was found to be a limiting factor for phytoplankton in general (*Chl-a*) and diatoms in particular in various frontal regions. However, the highest abundance of diatoms were associated with the regions of the Southern Ocean characterised by moderate wind speeds (10.2–11.3 m/s; Fig. 5) and intermediate PAR (21–25 E/m<sup>2</sup>/day; Figs 5 and 6). Wind speeds increase pole-ward and cause the intensification of upwelling, which is responsible for regulating the distribution of phytoplankton biomass (Arrigo *et al.* 1999; Sallee *et al.* 2010).

The influence of both wind speeds and PAR indicated the extensive variation in positive/negative trend of *Chl-a* and diatoms abundance during 1998–2012 (Fig. 5). It was observed that the diatoms abundance is under the purview of strong windier and turbulent environments and hence the dominance (96%) at PF over large spatial scales. Such impacts on diatoms trend from the STF to the SAF in an Indian sector of Southern Ocean was also reflected from inter annual variability of the Southern Annular Mode (SAM), which involves the intensification and southward migration of the Southern Ocean westerlies (Fig. 5), which may be the source (Bintanja *et al.* 2013) that effect shifting of the *Chl-a* and diatoms concentrations from STF to SAF and PF (Fig. 4).

This shift in the proportion of diatoms from STF to PF might be due to the some molecular mechanism known as genetic adaptability of the organisms. Therefore, the unique phytoplankton communities from subtropical to polar regions have the ability to utilize other environmental conditions to overcome

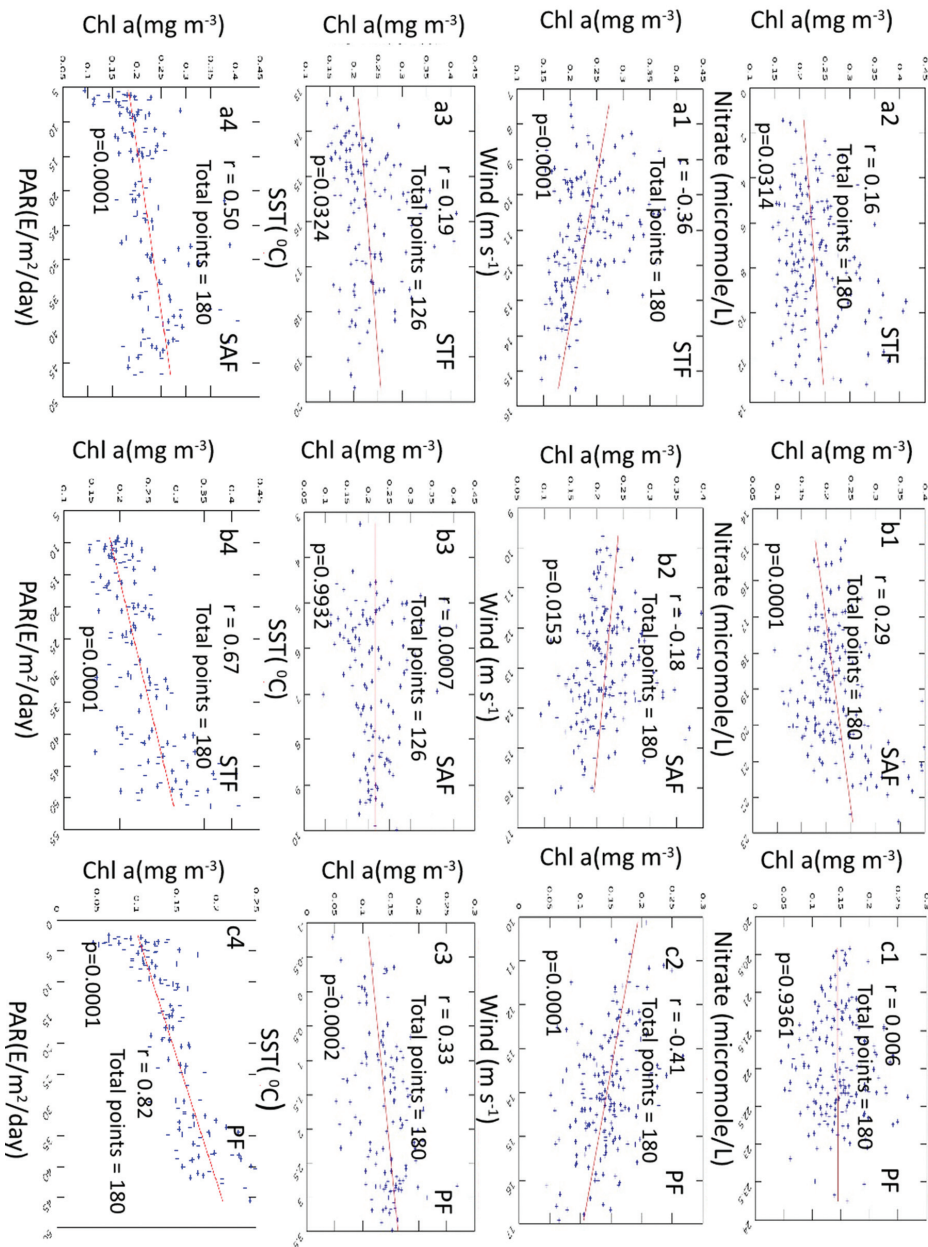


Fig. 6. Correlation between *Chl-a* and PAR, SST, wind and nitrate across the study area during 1998–2012, for the frontals STF (a1–a4), SAF (b1–b4) and PF (c1–c4).

the bioenergetics pressure (*i.e.* metabolic pathway) due to light, temperature, nutrients stratification, wind, oxygen minimum zones and carbonate saturation depth which regulate the spatial distribution (Barbara and Thomas 2014). Thus, the physical-chemical conditions might affect the adaptation of diatoms at the different fronts, as it was observed, maximum clustering over the SAF followed by the STF and PF.

The SST shows decreasing trend during 1998–2012 from STF to PF through SAF region with moderate variations (5.7°C–7.4°C). This trend may be caused due to the expansion of Antarctic sea ice, which is associated with decreasing SST and could explain the minimum variation at the PF. It is also consistent with global warming processes and associated expansion of Antarctica sea ice (Bintanja *et al.* 2013). In the present study it limits the area between 38°S–56°S, the heat flux induced SST cooling starts from STF and ends at PF coinciding a negative sea ice extent. As a result, the surface density at PF changes to form upper ocean stratification. The cross frontal phytoplankton bloom is detected near the marginal ice zone using *in-situ* and satellite observations in the Southern Ocean (Moore and Abbott 2002; Brusseler *et al.* 2003).

The reason for maximum diatoms abundance at the SAF and the PF compared to the STF may be due to the melting of sea ice, leading to water column stability, stratification, shallow mixed layer depth and input of iron, which acts as nutrient like iron as co-factor (Fitch and Moore 2007). Two important factors have been observed in the present study as restraining phytoplankton growth at the SAF and PF more than at STF, due to the iron limiting as the source of nutrient to surface waters through mixing or upwelling and the availability of irradiance (Arrigo *et al.* 1998). It has also been suggested elsewhere that the strong winds may possibly postpone the initiation of diatom concentrations, whereas moderate winds stimulate their growth. This is reflected (Fig. 5b1–b3) in the present modelled time series observations, where diatoms flourished mostly at the SAF during periods of average wind speeds, and gradually decline as winds get stronger. However, the greatest contribution of diatoms to *Chl-a* is seen at the PF and might be due to the impact of winds forcing for mixing (Fig. 5b1–5b3), low light adaptation and consumption of carbohydrate storage molecules (Morgan-Kiss *et al.* 2006). Furthermore, during the reduced irradiance period (Palmisano and Garrison 1993), diatoms can uptake dissolved organic material such as sugars and starches for energetic breakdown. In diatoms the urea cycle plays a major role as means of recovering carbon and nitrogen reduction during the duration of photo respiration (Parker *et al.* 2008), while in the presence of light, fatty acid (FA)- $\beta$ -oxidation pathway under which lipids can be used as metabolic intermediates for adenosine triphosphate (ATP) synthesis (Armbrust *et al.* 2004). Thus the metabolic plasticity being revealed through diatoms genomes is likely fundamental to their ability to flourish within extreme

and highly variable environments such as in the polar regions. Other authors have already reported that stratification, mixed layer depth and reduced winds regulate the phytoplankton composition, including diatoms (Fitch and Moore 2007; Gao *et al.* 2013). On the other hand, diatom intensifications are favoured during increased stratification due either to warm surface water or freshwater input. This is because diatoms prefer to live in not so well *i.e.* strong mixed waters (Arrigo *et al.* 1999). In another work, the integrated *Chl-a* concentration was highest at SAF south west region of SO (45°S) followed by STF and PF (Thomalla *et al.* 2011) and the diatoms dominance was 60% of the total phytoplankton biomass during 1996 and 2000. This result agrees with the present modelled observations where about 80% of the total *Chl-a* concentration was contributed by diatoms at both SAF and PF (Fig. 3).

PAR limitation has been reported as the cause of low phytoplankton biomass in the Southern Ocean (Mitchell *et al.* unpublished data). These findings support the present modelled time series observations (1998–2012), where at the surface of the PF with lowest PAR and high nitrate chlorophyll was low, whereas at the SAF with moderate PAR and moderate nitrate concentration *Chl-a* and diatoms showed maximum values (Figs 4 and 5). This moderate PAR and wind speeds along with the reduction of the extend of the MLD contributed to the larger phytoplankton production at the SAF than at the STF and the PF. On other hand, low PAR and high nitrate concentrations favoured diatoms dominance at the PF (Fig. 3b, c). Low light adapted diatoms efficiently utilized the available PAR and due to a genetic adaptability at SAF and PF (Fig. 6b3, c3). On the contrary, at the STF the maximum PAR correlates with SST (Fig. 6), where low *Chl-a* concentration could be due to the PAR exceeding photosynthetic requirements, causing photo-inhibition at the surface (Fig. 6a3).

## Conclusion

The highest *Chl-a* concentrations were observed at the SAF followed by the STF and PF, while the dominance of diatoms was evident at the PF followed by the SAF and the STF. It was shown that diatoms constitute more than 90% of the *Chl-a* at the PF and 86% at the SAF region, which indicates their tolerance to low light conditions and their ability to utilize carbohydrate storage molecules during low light periods. Modelled time series analysis of *Chl-a* and diatoms contribution to *Chl-a* during 1998–2012 show negative trends at the PF region. Further studies are required to analyse more *in-situ* observations along with biogeochemical models delineating phytoplankton functional types to better understand and compute the impact of changing diatoms contributions and other phytoplankton components on the biogeochemical cycles in the Indian Ocean sector of Southern Ocean.

**Acknowledgements.** — We greatly appreciate the Director of National Centre for Antarctic and Ocean Research (NCAOR) for his support and encouragement. Financial support from ESSO-MoES Project, SO biogeochemical studies is gratefully acknowledged. We thank the NASA-MODIS Project and NASA Ocean Biogeochemical Model for providing the satellite data, chlorophyll, PAR, SST, SSW for computational support and *in-situ* collection of nutrients, and phytoplankton sample by colleagues on board and the crew of the ORV *Sagar Nidhi* for their skilled cooperation and assistance during SOE-6 (2012) expedition. We would also like to thank two anonymous reviewers and the editor who had a great input to revise the manuscript and to bring into the current shape.

## Reference

- ABBOTT M.R., RICHMAN J.G., LETELIER R.M. and BARTLETT J.S. 2000. The spring bloom in the Antarctic Polar Frontal Zone as observed from a mesoscale array of bio-optical sensors. *Deep-Sea Research II* 47: 3285–3314.
- ARMBRUST E.V., BERGES J.A., BOWLER C., GREEN B.R., MARTINEZ D., PUTNAM N.H., ZHOU S.G., ALLEN A.E., APT K.E., BECHNER M., BRZEZINSKI M.A., CHAAL B.K., CHIOVITTI A., DAVIS A.K., DEMAREST M.S., DETTER J.C., GLAVINA T., GOODSTEIN D., HADI M.Z., HELLSTEN U., HILDEBRAND M., JENKINS B.D., JURKA J., KAPITONOV V.V., KRÖGER N., LAU W.W., LANE T.W., LARIMER F.W., LIPPMEIER J.C., LUCAS S., MEDINA M., MONTSANT A., OBORNICK M., PARKER M.S., PALENIK B., PAZOUR G.J., RICHARDSON P.M., RYNEARSON T.A., SAITO M.A., SCHWARTZ D.C., THAMATRAKOLN K., VALENTIN K., VARDI A., WILKERSON F.P. and ROKHSAR D.S. 2004. The genome of the diatom *Thalassiosira pseudonana*: ecology, evolution, and metabolism. *Science* 306: 79–86.
- ARMAND L.K., CROSTA X., ROMERO OSCAR E. and PICHON J.-J. 2005. The biogeography of major diatom taxa in Southern Ocean sediments: 1. Sea ice related species. *Palaeogeography, Palaeoclimatology, Palaeoecology* 223: 93–126.
- ARRIGO K.R., ROBINSON D.L., WARTHEN D.L., DUNBAR R.B., DITULLO G.R. and LIZATTE M.P. 1999. Phytoplankton community structure and the drawdown of nutrients and CO<sub>2</sub> in the Southern Ocean. *Science* 283: 365–367.
- ARRIGO K.R., WEISS A.M. and SMITH W.O. 1998. Physical forcing of phytoplankton dynamics in the western Ross Sea. *Journal of Geophysical Research* 103: 1007–1021.
- BARBARA R.L. and THOMAS M. 2014. Polar Microalgae: New approaches towards understanding adaptations to an extreme and changing environment. *Biology* 3: 56–80.
- BARLOW R., STUART V., LUTZ V., SESSIONS H., SATHYENDRANATH S., PLATT T., KYEWALYANGA M., CLEMENTSON L., FUKASAWA M., WATANABE S. and DEVRED E. 2007. Seasonal pigment patterns of surface phytoplankton in the subtropical southern hemisphere. *Deep-Sea Research I* 54: 1687–1703.
- BINTAGE R., OLDENBORGH G.J., DRIJFHOUT S.S., WOUTERS B. and KATSMAN C.A. 2013. Important role for ocean warming and increased ice-shelf melt in Antarctic sea-ice expansion. *Nature Geoscience* 6: 376–379.
- BROWN S.L. and LANDRY M.R. 2001. Microbial community structure and biomass in surface waters during a Polar Front summer bloom along 170° W. *Deep-Sea Research II* 48, 4039–4058.
- BUESSELER K.O., BARBER R.T., DICKSON M.-L., HISCOCOCK M.R., MOORE J.K. and SAMBROTTO R.N. 2003. The effect of marginal ice-edge dynamics on production and export in the Southern Ocean along 170 °W. *Deep-Sea Research II* 50: 579–603.

- FITCH D. and MOORE J.K. 2007. Wind speed influence on phytoplankton bloom dynamics in the Southern Ocean marginal ice zone. *Journal of Geophysical Research* 112: C08006.
- FURNAS M.J. 1991. Net in situ growth rates of phytoplankton in an oligotrophic, tropical shelf ecosystem. *Limnology and Oceanography* 36: 13–29.
- GAO Y., FAN S.M. and SARMIENTO J.L. 2003. Aeolian iron input to the ocean through precipitation scavenging: A modelling perspective and its implication for natural iron fertilization of the ocean. *Journal of Geophysical Research* 108: 4221.
- GAO S., WANG H., LIU G. and LI H. 2013. Spatio-temporal variability of chlorophyll *a* and its responses to sea surface temperature, winds and height anomaly in the western South China Sea. *Acta Oceanologica Sinica* 32: 48–58.
- GRASSHOFF K., EHRHARDT M. and KREMLING K. 1983. *Methods of seawater analysis*. 2 ed. Verlag Chemie, Weinheim: 419 pp.
- GREGG W.W., GINOUX P., SCHOPF P.S. and CASEY N.W. 2003. Phytoplankton and iron: validation of a global three-dimensional ocean biogeochemical model. *Deep-Sea Research II* 50: 3143–3169.
- HOLLIDAY N.P. and READ J.F. 1998. Surface oceanic fronts between Africa and Antarctica. *Deep-Sea Research I* 45: 217–238.
- HONJO S., MANGANINI S.J., KRISHFIELD R.A. and FRANCOIS R. 2008. Particulate organic carbon fluxes to the ocean interior and factors controlling the biological pump; a synthesis of global sediment trap programmes since 1983. *Progress in Oceanography* 76: 217–285.
- JENA B. 2016. Satellite remote sensing of Island mass effect on the sub-Antarctic Kerguelen Plateau, Southern Ocean. *Frontiers of Earth Science* 10: 479–486.
- KIRKMAN C.H. and BITZ C.M. 2011. The effect of the sea ice freshwater flux on Southern Ocean temperatures in CCSM3: Deep-ocean warming and delayed surface warming. *Journal of Climatology* 24: 2224–2237.
- MANN D.G. 1999. The species concept in diatoms. *Phycologia* 38: 437–495.
- MARTIN-JEZEQUEL H., HILDEBRAND M. and BRZEZINSKI M. 2000. Silicon metabolism in diatoms: Implications for growth. *Journal of Phycology* 36: 821–840.
- MENGELT C., ABBOTT M.R., BARTH J.A., LETELIER R.M., MEASURES C.I. and VINK S. 2001. Phytoplankton pigment distribution in relation to silicic acid, iron and the physical structure across the Antarctic Polar Front, 170°W, during austral summer. *Deep-Sea Research II* 48: 4081–4100.
- MISHRA R.K., Naik R.K. and Anilkumar N. 2015. Adaptations of phytoplankton in the Indian Ocean sector of the Southern Ocean during austral summer of 1998–2014. *Frontier Earth Science*. 2015 9: 742–752.
- MISHRA R.K., Jena B., Anilkumar N. and Sinha R.K. 2017. Shifting of phytoplankton community in the frontal regions of Indian Ocean sector of the Southern Ocean using in situ and satellite data. *Journal of Applied Remote Sensing* 1: 016019-1.
- MOORE J.K. and ABBOTT M.R. 2002. Surface chlorophyll concentrations in relation to the Antarctic Polar Front: seasonal and spatial patterns from satellite observations. *Journal of Marine System* 37: 69–86.
- MOORE J.K., DONEY S.C., KLEYPAS J.A., GLOVER D.M. and FUNG I.Y. 2002. Iron cycling and nutrient-limitation patterns in surface waters of the World Ocean. *Deep-Sea Research II* 49: 463–507.
- MORGAN-KISS R.M., PRISCU J.C., POCOCK T., SAVITCH L.G. and HUNER N.A. 2006. Adaptation and Acclimation of Photosynthetic Microorganisms to Permanently Cold Environments. *Microbiology and Molecular Biology Reviews* 70: 222–252.
- NELSON D.M., TRÉGUER P., BRZEZINSKI A., LAYNAERT A. and QUÉGUINER B. 1995. Production and dissolution of biogenic silica in the ocean: Revised global estimates, comparison with regional data and relationship to biogenic sedimentation. *Global Biogeochemical Cycle* 9: 359–372.

- ORSI A.H., WHITWORTH T. and NOWLIN W.D. 1995. On the meridional extent and fronts of the Antarctic Circumpolar Current. *Deep-Sea Research I* 42: 641–673.
- PARKER M.S., MOCK T. and ARMBRUST E.V. 2008. Genomic insights into marine microalgae. *Annual Review of Genetics* 42: 619–645.
- PALMISANO A.C. and GARRISON D.L. 1993. Microorganisms in Antarctic sea ice. *In*: E. Friedmann (ed.), *Antarctic microbiology* Wiley-Liss, New York: 167–218.
- SALAS M.F., ERIKSEN R., DAVIDSON A.T. and WRIGHT S.W. 2011. Protistan communities in the Australian sector of the Subantarctic Zone during SAZ-Sense. *Deep-Sea Research II* 49: 463–507.
- SALLEE J.B., SPEER K.G. and RINTOUL S.R. 2010. Zonally asymmetric response of the Southern Ocean mixed-layer depth to the Southern Annular Mode. *Nature Geoscience* 3: 273–279.
- SIGMAN D.M. and BOYLE E.A. 2000. Glacial/Interglacial variations in atmospheric carbon dioxide. *Nature* 407: 859–869.
- SIGMAN D.M., HAIN M.P. and HAUG G.H. 2010. The polar ocean and glacial cycles in atmospheric CO<sub>2</sub> concentration. *Nature* 466: 47–55.
- SMETACEK V., ASSMY P. and HENJES J. 2004. The role of grazing in structuring Southern Ocean pelagic ecosystems and biogeochemical cycles. *Antarctic Science* 16: 541–558.
- STOERMER E.F. and SMOL J.P. 1999. *The diatoms: Applications for the environmental and Earth Sciences*. Cambridge University Press, Cambridge: 469 pp.
- THOMALLA S., FAUCHEREAU N., SWART S. and MONTEIRO P. 2011. Regional scale characteristics of the seasonal cycle of chlorophyll in the Southern Ocean. *Biogeosciences* 8: 2849–2866.
- TREGUER P., NELSON D., VAN BENNEKOM A., DEMASTER D., LEYNAERT A. and QUEGUINER B. 1995. The silica balance in the world ocean: A reestimate. *Science* 268: 375–379.
- VAN HEUKELEM L.C. and THOMAS S. 2001. Computer-assisted high-performance liquid chromatography method development with applications to the isolation and analysis of phytoplankton pigments. *Journal of Chromatography* 910: 31–49.

Received 27 June 2016

Accepted 10 April 2017